Rib Bone Extraction Towards Liver Isolating in CT Scans Using Active Contour Segmentation Methods

Mahmoud S. Jawarneh[1], Shahid Munir Shah[2],
Mahmoud M. Aljawarneh[3], Ra'ed M. Al-Khatib[4], Mahmood G. Al-Bashayreh[5]
Faculty of Information Technology Applied Science Private University Amman, Jordan 11937[1,3,5]
Faculty of Eng. Sciences and Technology, Hamdard University, Karachi, Pakistan 74600[2]
Department of Computer Sciences, Yarmouk University, Irbid, Jordan 21163[4]

***Abstract*—Image segmentation is an important aspect of image processing and analysis. Medical imaging segmentation is critical for providing noninvasive information about human body structure that helps physicians analyze body anatomies efficiently. Until recently, various medical imaging segmentation approaches have been presented; however, these approaches are deficient in segmenting abdominal organs due to the significant similarity in their intensity levels. The purpose of this research is to propose a method to facilitate the segmentation of abdominal organs and improve the performance of the segmentation. The core functionality of this research is based on the extraction of rib bone from muscle tissues prior to the application of segmentation. This way, efficient segmentation of abdominal organs can be achieved by isolating the rib bone from the muscle tissues located between the rib bone. The proposed rib bone extraction mechanism is applied to four slices of the MICCAI2007 liver data set to isolate muscle tissues from liver tissues that have significant intensity similarity to liver tissues. The results indicate that the proposed extraction of rib bone efficiently isolated muscle tissues from linked liver tissues and improved the segmentation performance.**

***Keywords*—Active contour; computed tomography; segmentation; medical diagnostics; medical imaging segmentation**

I. Introduction

Image segmentation aims to partition an image into regions called segments used for further image analysis to achieve improved image compression efficiency and visualization effects [1], [2]. Image segmentation plays a vital role in medical imaging analysis for example providing noninvasive information about human body structure [3]. This information can support radiologists in visualizing and examining the anatomy of the body structure [4], tracking the progress of diseases [5], [6], [7], simulating biological processes [8], and evaluating the need for surgeries in radiotherapy [9], [10]. Threshold-based, region-growth-based, clustering-based, deformation-model based, machine learning (ML)-based, and active contour-based are different segmentation approaches that have been frequently employed in medical imaging analysis [11]. Medical imaging segmentation is important, yet it is a challenging task.

Most of the time, it requires manual delineation of organs by highly skilled personnel. Segmenting CT images is particularly complex compared to other medical imaging modalities. In such images, selecting each pixel of each slice manually could take hours or even days [12], [13]. Segmenting CT images of abdominal organs is more challenging because of their overlapping boundaries with the other organs (such as abdominal structure tissues and muscle tissues placed between rib bone). Most of the abdominal organs have similar intensity levels, which greatly affects the segmentation results of the methods based on intensity similarity [14]. Hence, methods based on gradient or intensity analysis are not feasible to segment images of abdominal organs [15]. Because of such limitations, most available segmentation methods, including active contour methods, fail to segment the abdominal tissues adjacent to the muscle tissues between rib bone [16], [17], [18]. Specific to the active contour segmentation methods, some existing approaches [19], [20], [21] adapted rib distance in the active contour level set formulation. This process slows the active contour segmentation since the contour curve takes longer to reach structural boundaries due to extra computations in the level set function.

Keeping in view the limitations of the existing studies, the following are the research questions that may be addressed during this research:

- How existing segmentation methods based on the intensity of the organs can segment the abdominal organs having similar intensity?
- How the efficiency of the existing segmentation method based on the intensity of the organs can be increased?

Extracting rib bone structures prior to applying the active contour method may facilitate the removal of intervening muscle tissues, thereby improving segmentation efficiency. The primary purpose of this research is to propose a method to facilitate the segmentation of abdominal organs with considerable similarity in intensity by performing rib bone extraction prior to active contour segmentation methods. The following are the objectives of the research:

- To improve the segmentation accuracy of the abdominal organs affected by the large similarity in intensity between abdominal structure tissues and muscle tissues located in between rib bone.
- To reduce the computation time while segmenting abdominal organs via active contour segmentation methods in the CT dataset. As a result, this leads to speeding up the processing time.

Based on the listed objectives, following are the contributions of the research:

- A rib bone extraction mechanism is proposed to efficiently segment the CT images of abdominal organs of similar intensity.
- The proposed rib bone extraction isolates the rib bone from the muscle tissues located in between the rib bone.
- The proposed rib bone extraction is specifically designed to be used prior to the application of "active contour" segmentation methods and has tested accordingly; however, it may be used prior to the application of any segmentation method.
- The proposed rib bone extraction has been applied to four MICCAI2007 Liver dataset [22], [23] slices to efficiently isolate liver tissues from muscle tissues with similar intensities.
- The proposed rib bone extraction simplifies the CT images and addresses the similarity of their intensity issue; hence, leads to a time and computationally efficient segmentation.
- The proposed approach is simple and easy to use, as well as applied prior to the application of the segmentation method(s). To the best of our knowledge, such an approach has never been proposed earlier, hence making it our novel contribution.

Based on the above listed research contributions, the following may be the advantages of the present study:

- The findings of the research will help clinicians efficiently segment, analyze, and visualize abdominal anatomies, as well as plan radiation therapy and surgery.
- The study's research findings will be used to assist software designers in constructing medical tools.
- The approach proposed in this study will help in teaching and research at medical schools.
- The methodologies and results proposed in this study will be useful in medical schools, teaching, and research.

The remainder of the paper is organized as follows: Section "Literature Review" explores and discusses reviewed literature in the area of medical imaging segmentation. Section "Material and Method" discusses the detailed methodology of the proposed method of extracting muscle tissues using the proposed rib bone extraction method before executing the active contour segmentation. "Results and Discussion" section discusses the results of the proposed method. Finally, "Conclusion and Future Direction" section presents the conclusion of the paper to highlight the contributions and findings along with possible future directions. A preprint of this manuscript has previously been published [24].

II. Related Work

Medical imaging segmentation has been a research focus from last few decades. During this time, a number of image segmentation techniques have been put forth to segment medical imaging for a range of applications, including the early diagnosis of disease, resource optimization, and maximizing efficiency of the existing systems etc. Image segmentation techniques include but not limited to; thresholding based [25], [26], [27], region growing based [28], [29], graph cut based [30], [31], shape model based [32], [33], edge detection based [34], [35], [36], clustering based [37], [38], [39], and more advanced ML [40], [41], [42], [43], and active contour-based methods [44], [45], [46]. In addition to significant contributions to image segmentation, particularly medical imaging segmentation, each proposed approach pose some limitations and challenges. For example, thresholding and region growing based methods are bound to use only image intensity or texture for the image segmentation [47], therefore, are failed to segment the organs with similar intensities. Graph-cut based methods are also limited in segmenting organs with overlapping tissues of similar intensities [31]. Shape based methods are heavily dependent on the training shapes, therefore, become time consuming processes for the images with large shape variations [48]. Recently, ML algorithms (specifically, Deep Learning (DL) algorithms), have emerged as efficient approaches for segmenting medical images [49], [50]. However, DL techniques frequently lack in understanding data and heavily rely on training data that has been manually labeled by medical professionals [48]. Furthermore, because of information loss in the consecutive down-sampling layers, some DL architectures, such as Convolutions Neural Network (CNN), perform poorly in comprehending precise object boundaries [51]. Also, in CNN architectures, 2D convolutions cannot completely utilize the spatial information along the third dimension [52], and 3D convolutions have a large memory consumption [53]. DL-based multi-organ segmentation techniques have also shown significant potential in medical imaging segmentation [54], and it has significantly improved the performance of the U-NET segmentation [55], however it is still challenging to obtain accurate and robust segmentation for the areas with ambiguous boundaries (such as abdominal organs) [56].

Supervised Machine Learning models such as Support Vector Machines (SVM) and Neural Networks (NN) have also shown reasonable performance in segmenting medical images, however, these methods are based on handcrafted and manually extracted features from the data, and for this heavily depend on the skills and experience of the researchers. Requirements of domain knowledge, extraction of features from data, and manual features engineering is basic hurdle to easily employ such algorithms [57], [49]. Active contour methods on the other hand have shown better performance to segment the complex gray-scale and variety of topological structures of medical images [58]. Because of their ability to provide closed and smooth contours of the target objects, these methods are one of the widely used segmentation methods today [59]. Many recent studies have reported to use active contour methods for different applications related to medical imaging segmentation [60], [61], [62], [63]. Although, active contour segmentation is one of the most attractive segmentations, however, in some cases it performs undesirably. For example, it performs poorly in segmenting complex natural images (without proper preprocessing) [64]. Furthermore, because of the susceptibility for intensity heterogeneity and boundary ambiguity of the input images, these methods fail to segment the abdominal tissues, especially tissues, which are adjacent to the muscle tissues between rib bone [65].

To address such limitation of the active contour methods, as a solution, combination of different strategies along with traditional active contour methods have been introduced by the researchers. For example, level set approach has been introduced with active contour to formulate it as energy minimization problem and then solving it with different strategies like gradient descent or partial differential equations [66]. Different DL architectures like CNN have also been combined with active contour to make it a more efficient hybrid segmentation methods [67]. Some of the studies have also introduced the combination of DL, level set, and active contours methods [68]. Such hybrid methodologies yielded good results but suffer with the time consumption issues because of the complexity of the training process. In short, introducing different strategies with traditional active contour methods, one way increases their segmentation capabilities, but on the other hand make them time consuming procedures. Furthermore, even with the latest proposed strategies, still the most existing active contour segmentation methods lack in segmenting the overlapping organs / region boundaries of the organs [69], [70], [71]. This study proposes that rib bone extraction be performed prior to active contour segmentation (refer to "Methodology" section for more information on the proposed method). The proposed approach is an effort to improve the accuracy of the active contour method(s) in particular and the other segmentation methods in general to segment abdominal organs (especially abdominal structure tissues and muscle tissues placed between rib bone) that have comparable intensity levels. Being not the actual part of the active contour, the proposed approach reduces the computation time of the active contour while segmenting abdominal organs. As a result, this leads to speeding up the processing time. Results show that with the help of the proposed approach, the active contour better segments abdominal organs (refer to Fig. 2) and achieves desirable performance in segmenting the organs of the similar intensity (refer to Section "Results and Discussion" for more details on the results achieved). The next section provides the comprehensive detail of the proposed rib bone extraction mechanisms along with the detail of the datasets used, experimentation performed, and the results obtained.

III. Material and Method

A. Proposed Approach

This study proposes that rib bone extraction be performed prior to active contour segmentation. This approach can be used to improve the accuracy of the active contour segmentation in particular and the other segmentation approaches in general in segmenting abdominal organs that have comparable intensity levels (i.e., abdominal structure tissues and muscle tissues placed between rib bone).

B. Methodology

Fig. 1 presents the overall flow diagram of the proposed rib bone extraction approach. According to Fig. 1, the proposed strategy of rib bone extraction is achieved through the following steps:

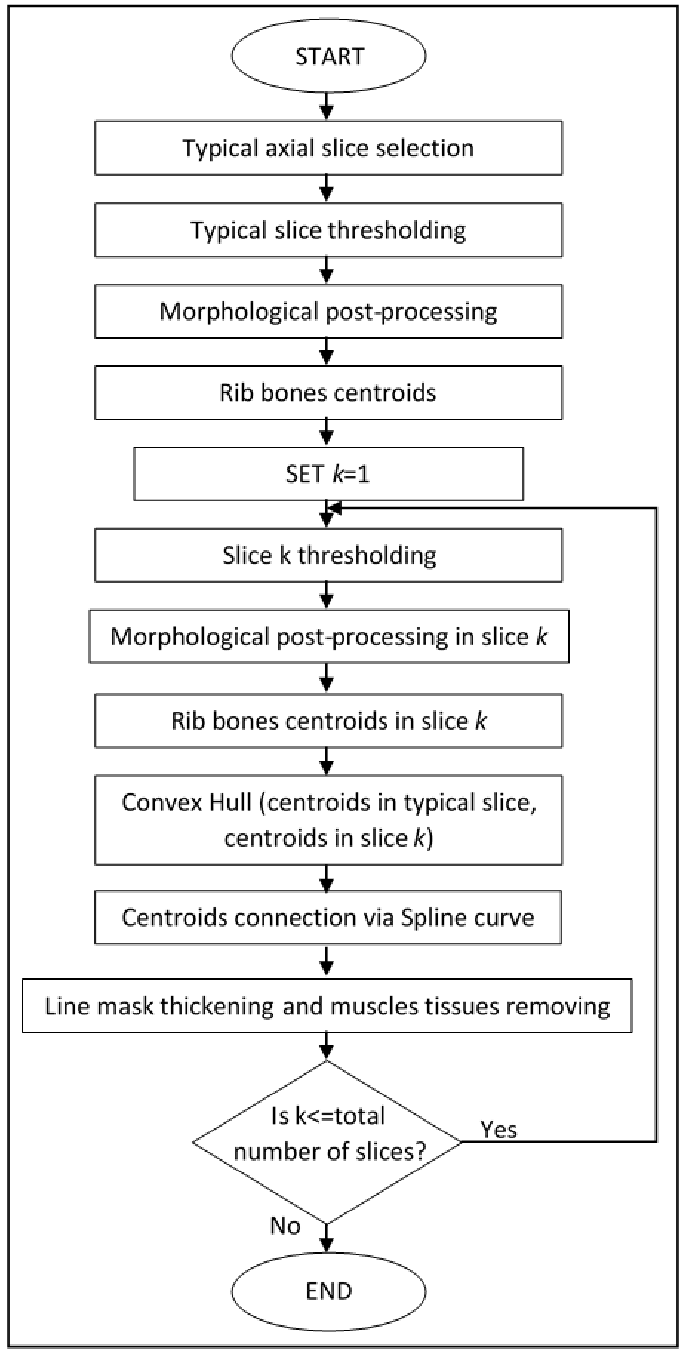

Fig. 1. Proposed rib bones extraction approach.

1) Typical slice of a CT image selection.
2) Performing thresholding on the selected typical slice to find rib bone in it.
3) Performing morphological post processing on the thresholded typical slice to eliminate the effects of thresholding on it.
4) Finding the centroids of each rib bone of the typical slice and saving them as cooperative knowledge for the other slices of the data.
5) Selecting the next slice (target slice) and finding the centroids of its rib bone using the centroid information of the typical slice.
6) Fitting the centroids of typical and target slices into convex hull function (to overcome the problem of the missing centroids).

7) Applying the spline curve method to connect the centroids and estimating the bone's boundary by a line.
8) Applying dilation morphological operation to thicken the estimated lined boundary.
9) Applying steps 5 to 8 above to every next slice by considering it a target slice until the slices of the whole data are finished.

An explanation of each of the above steps is provided in detail in the experimentation subsection.

C. Performance Evaluation

1) Evaluation based on Confusion Matrix: Performances of the proposed system has been measured in terms of accuracy, precision, sensitivity, and specificity provided using the confusion matrix. Table I presents the confusion matrix used to compute the performance measures. The outcomes of this confusion matrix are defined as:

True Positive (TP): The number of slices where muscles areas are removed as muscles areas.

False Positive (FP): The number of slices in which non-muscles areas are removed as muscles areas.

True Negative (TN): The number of slices where non-muscles areas are not removed as muscles areas.

False Negative (FN): The number of slices where muscles areas are not removed as muscles areas.

TABLE I. CONFUSION MATRIX FOR MUSCLE AREA CLASSIFICATION

	Yes	No
MUSCLES AREA	TP	FN
NON-MUSCLES AREA	FP	TN

The confusion matrix presented in Table I and four standard metrics for quantities evaluations are computed as follows:

$$\text{Accuracy} = \frac{TP + TN}{TP + TN + FP + FN} \tag{1}$$

$$\text{Precision} = \frac{TP}{TP + FP} \tag{2}$$

$$\text{Sensitivity} = \frac{TP}{TP + FN} \tag{3}$$

$$\text{Specificity} = \frac{TN}{TN + FP} \tag{4}$$

2) Evaluation based on 2D segmentation: In order to evaluate the proposed method, the method outputs need to be measured, analyzed and compared with manual segmentation. Therefore, the metrics must be carefully determined to accurately reflect the method performance in 2D segmentation performance. Dice coefficient (mean Index similarity) used to measure the accuracy of segmentation result for proposed method. The segmentation result of proposed method is termed AS and the gold standard is termed GT. The Dice coefficient DC (Dice, 1945) is one of the numbers of measures of the extent of spatial overlap between two segmented images. It is commonly used in reporting performance of segmentation and its values range between 0 if there is no overlap between the segmented region and the gold standard, and 1 for perfect agreement between the segmented region and the gold standard obtained using Eq. (5).

$$\text{DC} = \frac{2\,|AS \cap GT|}{|AS| + |GT|} \tag{5}$$

D. Experimentation

1) Dataset description: The proposed method was evaluated using four contrast-enhanced CT datasets from the Liver Segmentation Grand Challenge database. These datasets have a pixel resolution ranging from 0.55 mm to 0.8 mm, with inter-slice distances between 1 mm and 3 mm. Each axial slice consists of 512 x 512 pixels. The datasets, provided in Digital Imaging and Communications in Medicine (DICOM) format, have gray levels ranging from -1024 to +3071, corresponding to Hounsfield units (HU), the datasets accessed in 2024. The datasets used in this study—Liver1, Liver3, Liver4, and Liver6—contain 183, 79, 212, and 111 slices, respectively. However, the range of liver organ slice in each dataset shown in Table II.

TABLE II. ABDOMINAL ORGANS DATASETS

Abdominal Dataset Name	Dataset Source	Number of Slices	Range of Abdominal Organs Slices
Liver1	MICCAI2007	183	62–163
Liver3	MICCAI2007	79	14–70
Liver4	MICCAI2007	212	57–196
Liver6	MICCAI2007	111	20–92

2) Software detail: Image segmentation and statistical calculations are implemented in Matlab. The program is tested on a computer with Intel(R) Core(TM) i5-7200U CPU @ 2.50GHz 2.71 GHz, 4GB RAM, and Windows 10 Pro.

3) Rib bone extraction process: This section provides the detail of the proposed rib bone extraction approach along with the brief explanation of each step provided in the "proposed approach" subsection, and also shown the Fig. 1.

Fig. 2(a) illustrates the results of active contour segmentation before rib bone and muscle extraction, and Fig. 2(b) shows the result of active contour segmentation after rib bone and muscle extraction. It is clear from Fig. 2(a) and 2(b) that when rib bone extraction is performed prior to active contour segmentation, active contour segments the organs of similar intensity, i.e., abdominal organs, comparatively better than when rib bone extraction is not performed. This approach is the main idea our research.

It is well-known among radiology experts that some abdominal structures, especially the liver, are surrounded by rib bone. Therefore, their effective segmentation is difficult without rib bone extraction from their surroundings. Since the rib bone has the highest intensity in a CT dataset, simple binary thresholding may be applied to find the rib bone in it. In binary thresholding, images are converted from gray-scale or color images to binary images. Based on radiologists' knowledge, it is noted that there are some slices that don't have rib bone in all directions of the human body in the abdominal area, which leads to missing some of the muscle tissues. The proposed method thus finds the rib bone in a

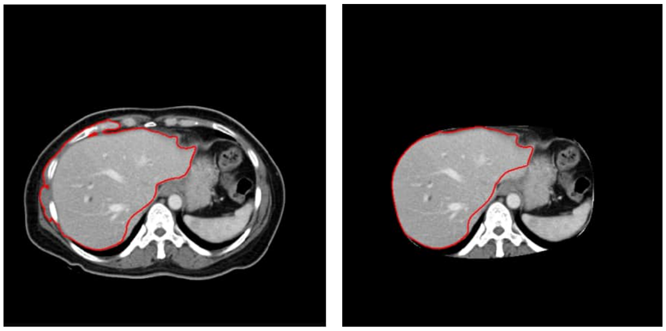

(a) Before bone extraction. (b) After bone extraction.

Fig. 2. Active contour segmentation before and after rib bone and muscle extraction from the abdominal organs of similar intensity.

typical slice chosen randomly from upper abdominal slices in the CT dataset, which have rib bone in all directions, as shown in Fig. 3, and applies binary thresholding on the chosen slice. Fig. 4(a) shows a typical slice in the upper abdominal region (upper view) and the result of thresholding in a typical slice shown in Fig. 4(b).

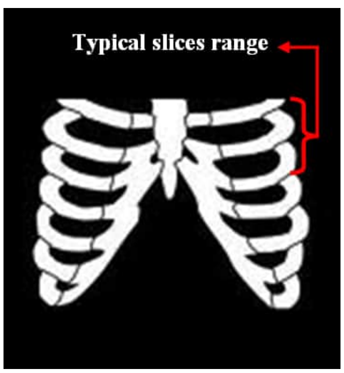

Fig. 3. A Typical slice chosen from the upper abdominal CT slices that have rib bones in all directions.

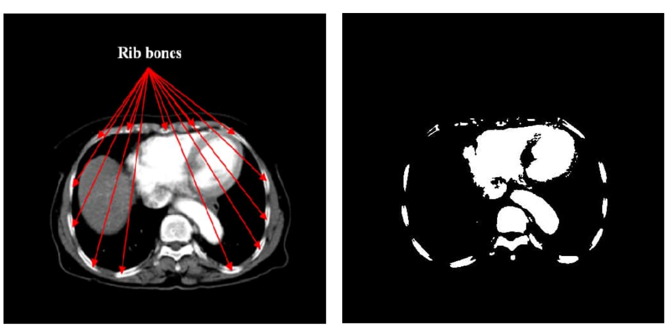

(a) Upper view of a typical slice in the upper abdominal region that has rib bones in all directions. (b) Upper view of the rib bone extraction after thresholding applied

Fig. 4. Typical slice.

It is evident from Fig 4(b) that, as a result of thresholding, the achieved rib bone is not well filled. Hence, a filling morphological operation is applied to fill the bone. The centroids of each rib are then computed. The centroids of ribs of the typical slice are saved temporarily to be used as a cooperative knowledge in the rib bone extraction for other remaining slices in the dataset. The rib bone extraction process is then applied to all slices in the abdominal dataset slice by slice with the following steps: To simplify the explanation, we refer to the slice under the rib bone extraction process as a target slice. Thresholding and filling morphological operations are applied to the target slice. The centroids of each rib bone in the target slice are obtained through region properties. Then the centroids of the typical slice and target slice are fitted into the convex hull function [72].

This function is used to find the appropriate arrangement in a clockwise cycle for these bones' centroids and take just the outer centroids. In some cases, some abdominal structures appear in white intensity, as shown in Fig. 5(a), which can affect the result of extracting ribs and muscles. However, the convex hull process overcomes those obstacles. In addition, the convex hull process also overcomes the problem of missing centroids in some directions by taking the centroids from a typical slice in the same directions. Fig. 5(a) shows an example of a target slice that does not have rib bones in all directions, and its thresholding result is shown in Fig. 5(b).

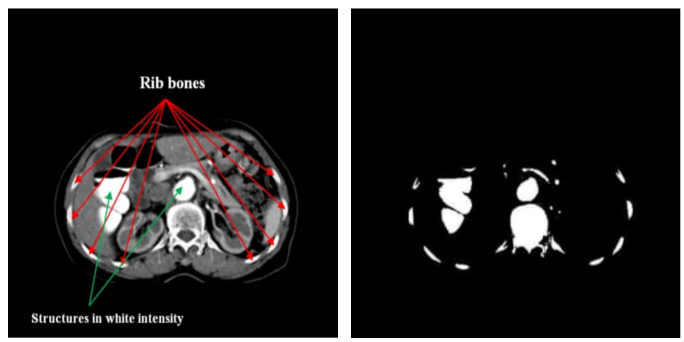

(a) Ribs in target slice. (b) Thresholding result.

Fig. 5. Target slice and its resultant slice after the application of thresholding.

The convex hull process is followed by the spline curve method to connect the centroids and estimate the bone's boundary. The connected points are then used to form a mask that isolates muscle tissues. Fig. 6 shows the line connecting the rib bones. The line connecting between the rib bones is then thickened by a dilation morphological operation (as shown in Fig. 7). The formed mask is applied to remove muscles located between rib bones.

This operation aims to remove the rib bones and muscles, which solve the problem of intensity similarity with abdominal structure tissues. Fig. 8 shows removing ribs and muscles. Choosing an appropriate thickening for connecting line is an essential factor that affects the accuracy of segmentation results. We choose an appropriate thickening value through experiments. Fig. 9 shows the effect of line mask thickening size; if the mask line thickened uses a bigger value, the mask will isolate some of the abdominal structure tissues, as shown in Fig. 9(b). If the mask line thickened to an appropriate size, the mask will isolate rib bones and muscles tissue only, as shown in Fig. 9(a).

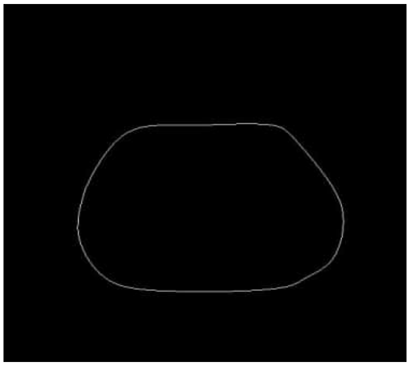

Fig. 6. Line connected between ribs.

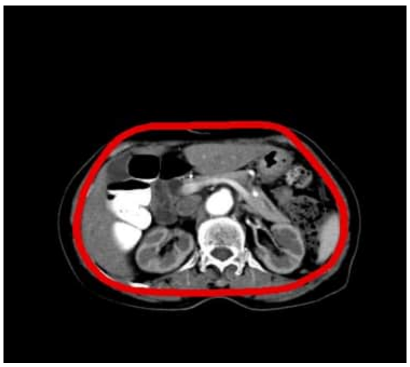

Fig. 7. Line thickening by the application of dilation morphological operation.

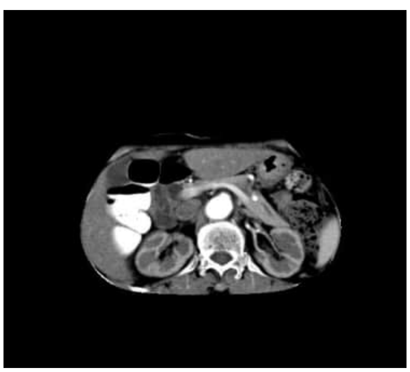

Fig. 8. Removal of rib bones from muscles.

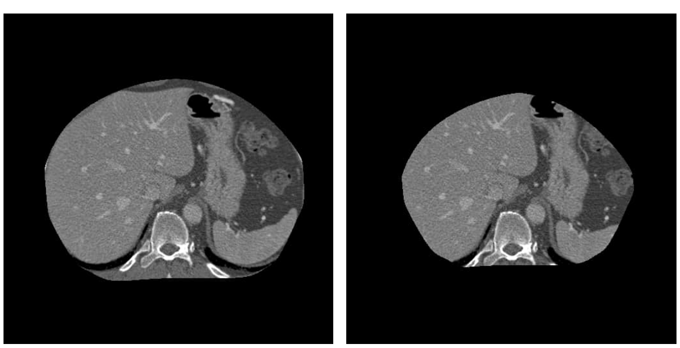

(a) Appropriate thickening. (b) Big thickening.

Fig. 9. Effects of line thickening on rib bone and muscles separation.

Rib bones extraction is applied to four MICCAI2007 Liver datasets [22], [23] (liver1, liver3, liver4, and liver6) slices to isolate muscle tissues that have significant intensity similarity with liver tissues. Fig. 10 shows rib bone extraction for some slices in these datasets [i.e. Fig. 10(a) (slice 151 Liver1), Fig. 10(b) (slice 61 Liver3), Fig. 10(c) (slice 158 Liver4), and Fig. 10(d) (slice 64 Liver6)]. Rib bones extraction is not performed on the Liver5 dataset due to the clear distinction in intensity between the liver tissue and muscles tissue.

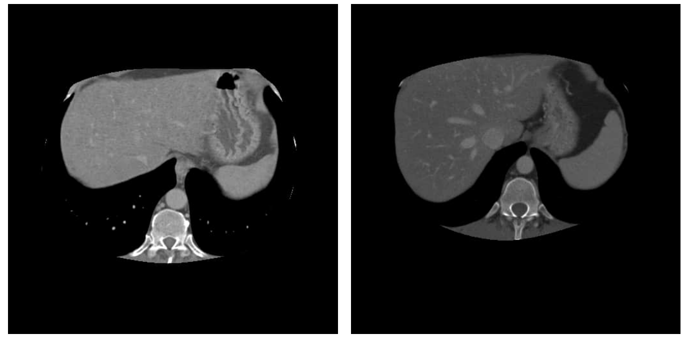

(a) Slice 151 Liver1 (b) Slice 61 Liver3

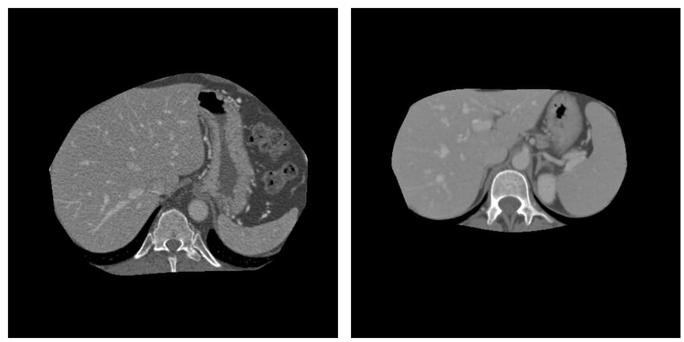

(c) Slice 158 Liver4 (d) Slice 64 Liver6

Fig. 10. Rib bones extraction applied to four MICCAI2007 Liver datasets i.e. liver1, liver3, liver4, and liver6.

IV. Results and Discussion

A. Results Based on Confusion Matrix

Table III shows the evaluations quantities for each Liver data set and the weighted average performance where the weights correspond to the number of slices in each dataset. Results presented in Table III indicates that the proposed approach has efficiently extracted the rib bones from the slices of the Liver dataset.

TABLE III. Quantitative Evaluations for Rib Bone Extraction

Dataset	Slices Number	Accuracy	Precision	Sensitivity	Specificity
liver1	102	0.83	0.80	0.96	0.78
liver3	57	0.86	0.82	0.93	0.79
liver4	140	0.92	0.88	0.96	0.87
liver6	73	0.84	0.92	0.75	0.93
Average	-	0.87	0.86	0.91	0.84

Fig. 11 [Fig. 11(a) (original slice), and Fig. 11(b) (muscles isolating)] shows an example of a true positive (TP) case where the muscle tissue between rib bones is isolated completely.

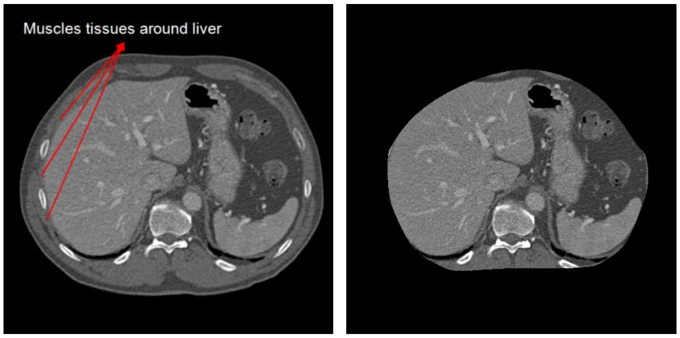

(a) Original slice (b) Muscles isolating

Fig. 11. A true positive case where the muscle tissue between rib bones is isolated completely from muscles.

Fig. 12 [Fig. 12(a) (original slice), and Fig. 12(b) (pieces removed)] shows an example of a false positive (FP) case where some parts of liver tissues (non-muscle tissues) are removed as a muscle area. From rib bone extraction results, it can be noted that the efficiency of this method is acceptable.

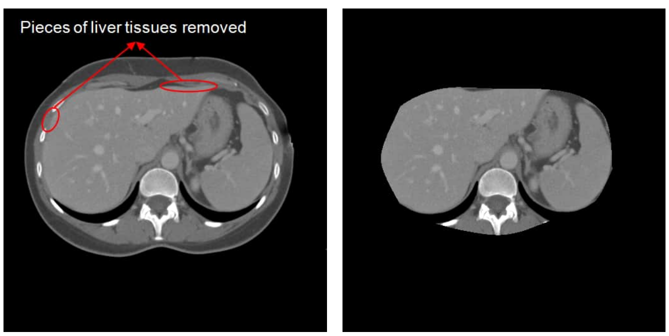

(a) Original slice (b) Pieces removed

Fig. 12. A false positive case where some parts of liver tissues are removed as muscle.

B. Results Based on Dice Coefficient

Table IV shows the mean Dice coefficient values in all datasets, all slices for each liver organ. Fig. 13 (a)–(d) show the results of the Dice coefficient for the liver regions in the four MICCAI2007 liver datasets (Liver1, Liver3, Liver4 and Liver6).

TABLE IV. QUANTITATIVE MEASURES FOR FOUR LIVER ORGAN DATASETS

Dataset	Number of Segmented Liver Slices	Mean Dice Coefficient
Liver1	102	0.88
Liver3	57	0.90
Liver4	140	0.92
Liver6	73	0.90
Average	–	0.90

The quantitative measures presented in Fig. 13 and Table IV, shows a positive correlation and high similarity between the proposed method and the experts' manual segmentation, reflected by the mean of Dice coefficient for all four liver organs (0.90).

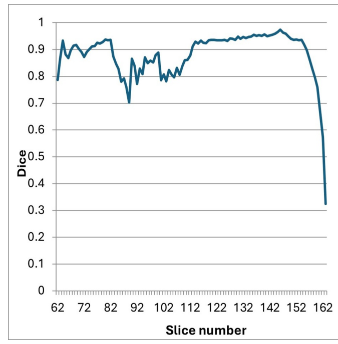

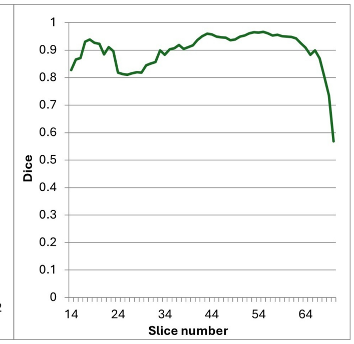

(a) Liver1 (b) Liver3

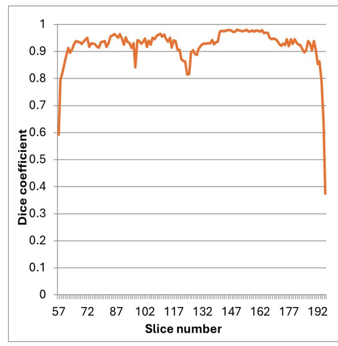

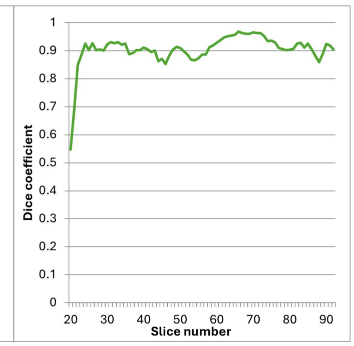

(c) Liver4 (d) Liver6

Fig. 13. Dice coefficient for four liver organs: Proposed method versus manual segmentation.

Finally, the results achieved in this study are compared with the state of-the-art active contour-based segmentation methods in the literature i.e. [71], [73]. As Compared to [71], [73] our proposed model achieved promising results in terms of precision, recall, and f-measures scores.

V. CONCLUSION AND FUTURE DIRECTIONS

In this research, a rib bone extraction mechanism is proposed to be used prior to segmentation methods such as active contour to segment abdominal organs of similar intensity. Similar intensity of abdominal organs, such as abdominal structure tissues and muscle tissues located in between rib bone, greatly affects the performance of the segmentation methods, and most available segmentation approaches based on intensity of the organs, fail to efficiently segment these organs. The proposed rib bone extraction is used to isolate muscle tissues that have similar intensity with abdominal structure tissues; hence, it makes the segmentation process computationally efficient and simpler to use. The rib bone extraction mechanism isolates muscle tissues with a large degree of similarity in their intensity with the abdominal structure. Consequently, this prevents the active contour curve from leaking into muscle tissues during the segmentation process. The proposed rib bone extraction is applied on four MICCAI2007 Liver data set [22], [23] slices to isolate muscle tissues from liver tissues that have significant similarity in intensity with liver tissues. Results indicate that the proposed rib bone extraction approach has efficiently isolated muscle tissues from the linked liver tissues.

The proposed rib bone extraction is specifically designed to be used prior to the application of "active contour" segmentation methods and has been tested accordingly; however, it may be used prior to the application of any segmentation method.

In future, this method will be tested with the other state-of-the-art segmentation approaches to check its suitability with these methods and to better validate our hypothesis.

Data Availability

MICCAI2007 data were used to support this study and are available at https://www.semanticscholar.org/paper/Semi-automatic-Segmentation-of-the-Liver-and-its-onDawantLi/bacf1b9ffec68f01d93d6389faea03432060e07d. These prior studies (and datasets) are cited at relevant places within the text as reference [22], [23].

References

[1] R. E Woods and R. C Gonzalez, "Digital image processing," 2008.

[2] R. Klette, *Concise computer vision*. Springer, 2014, vol. 233.

[3] A. S. Ashour, Y. Guo, and W. S. Mohamed, *Thermal Ablation Therapy: Theory and Simulation*. Academic Press, 2021.

[4] A. A. Farag, M. N. Ahmed, A. El-Baz, and H. Hassan, "Advanced segmentation techniques," *Handbook of Biomedical Image Analysis: Volume I: Segmentation Models Part A*, vol. 1, pp. 479–533, 2005.

[5] A. Khan, R. Garner, M. L. Rocca, S. Salehi, and D. Duncan, "A novel threshold-based segmentation method for quantification of covid-19 lung abnormalities," *Signal, image and video processing*, vol. 17, no. 4, pp. 907–914, 2023.

[6] V. Grau, A. Mewes, M. Alcaniz, R. Kikinis, and S. K. Warfield, "Improved watershed transform for medical image segmentation using prior information," *IEEE transactions on medical imaging*, vol. 23, no. 4, pp. 447–458, 2004.

[7] H. Greenspan, A. Ruf, and J. Goldberger, "Constrained gaussian mixture model framework for automatic segmentation of mr brain images," *IEEE transactions on medical imaging*, vol. 25, no. 9, pp. 1233–1245, 2006.

[8] M. Prastawa, E. Bullitt, and G. Gerig, "Simulation of brain tumors in mr images for evaluation of segmentation efficacy," *Medical image analysis*, vol. 13, no. 2, pp. 297–311, 2009.

[9] M. Astaraki, M. Severgnini, V. Milan, A. Schiattarella, F. Ciriello, M. de Denaro, A. Beorchia, and H. Aslian, "Evaluation of localized region-based segmentation algorithms for ct-based delineation of organs at risk in radiotherapy," *Physics and Imaging in Radiation Oncology*, vol. 5, pp. 52–57, 2018.

[10] M. Y. Ansari, A. Abdalla, M. Y. Ansari, M. I. Ansari, B. Malluhi, S. Mohanty, S. Mishra, S. S. Singh, J. Abinahed, A. Al-Ansari *et al.*, "Practical utility of liver segmentation methods in clinical surgeries and interventions," *BMC medical imaging*, vol. 22, no. 1, pp. 1–17, 2022.

[11] A. S. El-Baz, R. Acharya, M. Mirmehdi, and J. S. Suri, *Multi Modality State-of-the-Art Medical Image Segmentation and Registration Methodologies: Volume 1*. Springer Science & Business Media, 2011, vol. 1.

[12] E. Casiraghi, P. Campadelli, S. Pratissoli, and G. Lombardi, "Automatic abdominal organ segmentation from ct images," *ELCVIA Electronic Letters on Computer Vision and Image Analysis*, vol. 8, no. 1, pp. 1–14, 2009.

[13] M. S. Jawarneh and M. S. Abual-Rub, "Knowledge-based system guided automatic contour segmentation of abdominal structures in ct scans," *International Journal of Intelligent Information Systems*, vol. 5, no. 1, pp. 5–16, 2016.

[14] A. E. Kavur, N. S. Gezer, M. Barış, S. Aslan, P.-H. Conze, V. Groza, D. D. Pham, S. Chatterjee, P. Ernst, S. Özkan *et al.*, "Chaos challenge-combined (ct-mr) healthy abdominal organ segmentation," *Medical Image Analysis*, vol. 69, p. 101950, 2021.

[15] C. Li, X. Wang, S. Eberl, M. Fulham, Y. Yin, and D. Feng, "Fully automated liver segmentation for low-and high-contrast ct volumes based on probabilistic atlases," in *2010 IEEE International Conference on Image Processing*. IEEE, 2010, pp. 1733–1736.

[16] S. Pan and B. M. Dawant, "Automatic 3d segmentation of the liver from abdominal ct images: a level-set approach," in *Medical Imaging 2001: Image Processing*, vol. 4322. SPIE, 2001, pp. 128–138.

[17] N. K. Lee, H. Sowa, E. Hinoi, M. Ferron, J. D. Ahn, C. Confavreux, R. Dacquin, P. J. Mee, M. D. McKee, D. Y. Jung *et al.*, "Endocrine regulation of energy metabolism by the skeleton," *Cell*, vol. 130, no. 3, pp. 456–469, 2007.

[18] J. F. Garamendi, N. Malpica, J. Martel, and E. Schiavi, "Automatic segmentation of the liver in ct using level sets without edges," in *Pattern Recognition and Image Analysis: Third Iberian Conference, IbPRIA 2007, Girona, Spain, June 6-8, 2007, Proceedings, Part I 3*. Springer, 2007, pp. 161–168.

[19] T. Furukawa, M. Maekawa, T. Oki, I. Suda, S. Iida, H. Shimada, I. Takamure, and K.-i. Kadowaki, "The rc and rd genes are involved in proanthocyanidin synthesis in rice pericarp," *The Plant Journal*, vol. 49, no. 1, pp. 91–102, 2007.

[20] J. S. Athertya and G. S. Kumar, "Automatic segmentation of vertebral contours from ct images using fuzzy corners," *Computers in biology and medicine*, vol. 72, pp. 75–89, 2016.

[21] J. Yang, R. Shi, L. Jin, X. Huang, K. Kuang, D. Wei, S. Gu, J. Liu, P. Liu, Z. Chai *et al.*, "Deep rib fracture instance segmentation and classification from ct on the ribfrac challenge," *arXiv preprint arXiv:2402.09372*, 2024.

[22] B. M. Dawant, R. Li, B. Lennon, and S. Li, "Semi-automatic segmentation of the liver and its evaluation on the miccai 2007 grand challenge data set," *3D Segmentation in The Clinic: A Grand Challenge*, pp. 215–221, 2007.

[23] L. Jin, S. Gu, D. Wei, J. K. Adhinarta, K. Kuang, Y. J. Zhang, H. Pfister, B. Ni, J. Yang, and M. Li, "Ribseg v2: A large-scale benchmark for rib labeling and anatomical centerline extraction," *IEEE Transactions on Medical Imaging*, vol. 43, no. 1, pp. 570–581, 2023.

[24] M. S. Jawarneh, S. M. Shah, M. M. Aljawarneh, R. M. Al-Khatib, and M. G. Al-Bashayreh, "Rib bone extraction towards liver isolating in ct scans using active contour segmentation methods."

[25] Y. Feng, H. Zhao, X. Li, X. Zhang, and H. Li, "A multi-scale 3d otsu thresholding algorithm for medical image segmentation," *Digital Signal Processing*, vol. 60, pp. 186–199, 2017.

[26] M. Abdel-Basset, V. Chang, and R. Mohamed, "A novel equilibrium optimization algorithm for multi-thresholding image segmentation problems," *Neural Computing and Applications*, vol. 33, pp. 10 685–10 718, 2021.

[27] E. H. Houssein, B. E.-d. Helmy, D. Oliva, A. A. Elngar, and H. Shaban, "A novel black widow optimization algorithm for multilevel thresholding image segmentation," *Expert Systems with Applications*, vol. 167, p. 114159, 2021.

[28] N. Mesanovic, M. Grgic, H. Huseinagic, M. Males, E. Skejic, and M. Smajlovic, "Automatic ct image segmentation of the lungs with region growing algorithm," in *18th international conference on systems, signals and image processing-IWSSIP*, 2011, pp. 395–400.

[29] X. Zhang, X. Li, and Y. Feng, "A medical image segmentation algorithm based on bi-directional region growing," *Optik*, vol. 126, no. 20, pp. 2398–2404, 2015.

[30] H. Zhou, J. Zheng, and L. Wei, "Texture aware image segmentation using graph cuts and active contours," *Pattern Recognition*, vol. 46, no. 6, pp. 1719–1733, 2013.

[31] X. Lu, Q. Xie, Y. Zha, and D. Wang, "Fully automatic liver segmentation combining multi-dimensional graph cut with shape information in 3d ct images," *Scientific reports*, vol. 8, no. 1, p. 10700, 2018.

[32] S. Dambreville, Y. Rathi, and A. Tannenbaum, "A framework for image segmentation using shape models and kernel space shape priors," *IEEE transactions on pattern analysis and machine intelligence*, vol. 30, no. 8, pp. 1385–1399, 2008.

[33] M. Esfandiarkhani and A. H. Foruzan, "A generalized active shape model for segmentation of liver in low-contrast ct volumes," *Computers in Biology and Medicine*, vol. 82, pp. 59–70, 2017.

[34] S. S. Al-Amri, N. Kalyankar, and S. Khamitkar, "Image segmentation by using edge detection," *International journal on computer science and engineering*, vol. 2, no. 3, pp. 804–807, 2010.

[35] R. Muthukrishnan and M. Radha, "Edge detection techniques for image segmentation," *International Journal of Computer Science & Information Technology*, vol. 3, no. 6, p. 259, 2011.

[36] A. Aslam, E. Khan, and M. S. Beg, "Improved edge detection algorithm for brain tumor segmentation," *Procedia Computer Science*, vol. 58, pp. 430–437, 2015.

[37] N. Dhanachandra, K. Manglem, and Y. J. Chanu, "Image segmentation using k-means clustering algorithm and subtractive clustering algorithm," *Procedia Computer Science*, vol. 54, pp. 764–771, 2015.

[38] E. Abdel-Maksoud, M. Elmogy, and R. Al-Awadi, "Brain tumor segmentation based on a hybrid clustering technique," *Egyptian Informatics Journal*, vol. 16, no. 1, pp. 71–81, 2015.

[39] N. Dhanachandra and Y. J. Chanu, "A survey on image segmentation methods using clustering techniques," *European Journal of Engineering and Technology Research*, vol. 2, no. 1, pp. 15–20, 2017.

[40] M. Hatt, C. Parmar, J. Qi, and I. El Naqa, "Machine (deep) learning methods for image processing and radiomics," *IEEE Transactions on Radiation and Plasma Medical Sciences*, vol. 3, no. 2, pp. 104–108, 2019.

[41] T. Zhou, S. Ruan, and S. Canu, "A review: Deep learning for medical image segmentation using multi-modality fusion," *Array*, vol. 3, p. 100004, 2019.

[42] M. H. Hesamian, W. Jia, X. He, and P. Kennedy, "Deep learning techniques for medical image segmentation: achievements and challenges," *Journal of digital imaging*, vol. 32, pp. 582–596, 2019.

[43] S. Chaudhury, A. N. Krishna, S. Gupta, K. S. Sankaran, S. Khan, K. Sau, A. Raghuvanshi, and F. Sammy, "Effective image processing and segmentation-based machine learning techniques for diagnosis of breast cancer," *Computational and Mathematical Methods in Medicine*, vol. 2022, 2022.

[44] L. Fang, X. Wang, and L. Wang, "Multi-modal medical image segmentation based on vector-valued active contour models," *Information sciences*, vol. 513, pp. 504–518, 2020.

[45] B. Han and Y. Wu, "Active contour model for inhomogenous image segmentation based on jeffreys divergence," *Pattern Recognition*, vol. 107, p. 107520, 2020.

[46] A. S. Abdullah, J. Rahebi, Y. E. Özok, and M. Aljanabi, "A new and effective method for human retina optic disc segmentation with fuzzy clustering method based on active contour model," *Medical & biological engineering & computing*, vol. 58, pp. 25–37, 2020.

[47] J.-l. Fan and F. Zhao, "Two-dimensional otsu's curve thresholding segmentation method for gray-level images," *Acta Electonica Sinica*, vol. 35, no. 4, p. 751, 2007.

[48] Y. Gao, Y. Shao, J. Lian, A. Z. Wang, R. C. Chen, and D. Shen, "Accurate segmentation of ct male pelvic organs via regression-based deformable models and multi-task random forests," *IEEE transactions on medical imaging*, vol. 35, no. 6, pp. 1532–1543, 2016.

[49] S. M. Shah, R. A. Khan, S. Arif, and U. Sajid, "Artificial intelligence for breast cancer analysis: Trends & directions," *Computers in Biology and Medicine*, vol. 142, p. 105221, 2022.

[50] U. Sajid, R. A. Khan, S. M. Shah, and S. Arif, "Breast cancer classification using deep learned features boosted with handcrafted features," *Biomedical Signal Processing and Control*, vol. 86, p. 105353, 2023.

[51] M. Zhang, B. Dong, and Q. Li, "Deep active contour network for medical image segmentation," in *Medical Image Computing and Computer Assisted Intervention–MICCAI 2020: 23rd International Conference, Lima, Peru, October 4–8, 2020, Proceedings, Part IV 23*. Springer, 2020, pp. 321–331.

[52] P. F. Christ, M. E. A. Elshaer, F. Ettlinger, S. Tatavarty, M. Bickel, P. Bilic, M. Rempfler, M. Armbruster, F. Hofmann, M. D'Anastasi *et al.*, "Automatic liver and lesion segmentation in ct using cascaded fully convolutional neural networks and 3d conditional random fields," in *International conference on medical image computing and computer-assisted intervention*. Springer, 2016, pp. 415–423.

[53] K. Simonyan and A. Zisserman, "Very deep convolutional networks for large-scale image recognition," 2015.

[54] Y. Fu, Y. Lei, T. Wang, W. J. Curran, T. Liu, and X. Yang, "A review of deep learning based methods for medical image multi-organ segmentation," *Physica Medica*, vol. 85, pp. 107–122, 2021.

[55] M. Bardis, R. Houshyar, C. Chantaduly, A. Ushinsky, J. Glavis-Bloom, M. Shaver, D. Chow, E. Uchio, and P. Chang, "Deep learning with limited data: organ segmentation performance by u-net," *Electronics*, vol. 9, no. 8, p. 1199, 2020.

[56] H. Lin, Z. Li, Z. Yang, and Y. Wang, "Variance-aware attention u-net for multi-organ segmentation," *Medical Physics*, vol. 48, no. 12, pp. 7864–7876, 2021.

[57] J. Waring, C. Lindvall, and R. Umeton, "Automated machine learning: Review of the state-of-the-art and opportunities for healthcare," *Artificial intelligence in medicine*, vol. 104, p. 101822, 2020.

[58] S. Yin, H. Li, D. Liu, and S. Karim, "Active contour modal based on density-oriented birch clustering method for medical image segmentation," *Multimedia Tools and Applications*, vol. 79, pp. 31 049–31 068, 2020.

[59] M. Saeidifar, M. Yazdi, and A. Zolghadrasli, "Performance improvement in brain tumor detection in mri images using a combination of evolutionary algorithms and active contour method," *Journal of Digital Imaging*, vol. 34, pp. 1209–1224, 2021.

[60] E. Carbajal-Degante, S. Avendaño, L. Ledesma, J. Olveres, E. Vallejo, and B. Escalante-Ramirez, "A multiphase texture-based model of active contours assisted by a convolutional neural network for automatic ct and mri heart ventricle segmentation," *Computer Methods and Programs in Biomedicine*, vol. 211, p. 106373, 2021.

[61] H. Lv, F. Zhang, and R. Wang, "Robust active contour model using patch-based signed pressure force and optimized fractional-order edge," *IEEE Access*, vol. 9, pp. 8771–8785, 2021.

[62] Y. Zhang, J. Duan, Y. Sa, and Y. Guo, "Multi-atlas based adaptive active contour model with application to organs at risk segmentation in brain mr images," *IRBM*, vol. 43, no. 3, pp. 161–168, 2022.

[63] G. Wang, F. Zhang, Y. Chen, G. Weng, and H. Chen, "An active contour model based on local pre-piecewise fitting bias corrections for fast and accurate segmentation," *IEEE Transactions on Instrumentation and Measurement*, vol. 72, pp. 1–13, 2023.

[64] P. Xue and S. Niu, "A novel active contour model based on feature for image segmentation."

[65] J.-A. Pérez-Carrasco, C. Serrano, and B. Acha, "Automatic segmentation of bone and muscle structures in ct volumes using convex relaxation and fine-tuning," in *XV Mediterranean Conference on Medical and Biological Engineering and Computing–MEDICON 2019: Proceedings of MEDICON 2019, September 26-28, 2019, Coimbra, Portugal*. Springer, 2020, pp. 397–404.

[66] Y. Chen, P. Ge, G. Wang, G. Weng, and H. Chen, "An overview of intelligent image segmentation using active contour models," *Intell. Robot.*, vol. 3, no. 1, pp. 23–55, 2023.

[67] C. Rupprecht, E. Huaroc, M. Baust, and N. Navab, "Deep active contours," 2016.

[68] S. Gur, T. Shaharabany, and L. Wolf, "End to end trainable active contours via differentiable rendering," 2019.

[69] J. Chu, Y. Chen, W. Zhou, H. Shi, Y. Cao, D. Tu, R. Jin, and Y. Xu, "Pay more attention to discontinuity for medical image segmentation," in *Medical Image Computing and Computer Assisted Intervention–MICCAI 2020: 23rd International Conference, Lima, Peru, October 4–8, 2020, Proceedings, Part IV 23*. Springer, 2020, pp. 166–175.

[70] R. Jin and G. Weng, "A robust active contour model driven by pre-fitting bias correction and optimized fuzzy c-means algorithm for fast image segmentation," *Neurocomputing*, vol. 359, pp. 408–419, 2019.

[71] X. Shu, Y. Yang, J. Liu, X. Chang, and B. Wu, "Alvls: Adaptive local variances-based levelset framework for medical images segmentation," *Pattern Recognition*, vol. 136, p. 109257, 2023.

[72] M. Jayaram and H. Fleyeh, "Convex hulls in image processing: a scoping review," *American Journal of Intelligent Systems*, vol. 6, no. 2, pp. 48–58, 2016.

[73] G. Harini, A. Farooq, and D. Mishra, "Leveraging auxiliary classification for rib fracture segmentation," *arXiv e-prints*, pp. arXiv–2411, 2024.